New Alternative Donor−Acceptor Arranged Poly(Aryleneethynylene)s and Their Related Compounds Composed of Five-Membered Electron-Accepting 1,3,4-Thiadiazole, 1,2,4-Triazole, or 3,4-Dinitrothiophene Units: Synthesis, Packing Structure, and Optical Properties

Takuma Yasuda,[†] Tatsuya Imase,[‡] Yoshiyuki Nakamura,[†] and Takakazu Yamamoto*,[†]

Chemical Resources Laboratory, Tokyo Institute of Technology, 4259 Nagatsuta, Midori-ku, Yokohama 226-8503, Japan and Department of Electronic Chemistry, Interdisciplinary Graduate School of Science and Engineering, Tokyo Institute of Technology, 4259 Nagatsuta, Midori-ku, Yokohama 226-8503, Japan

Received February 24, 2005; Revised Manuscript Received April 3, 2005

ABSTRACT: A series of new poly(aryleneethynylene)-type π-conjugated copolymers, which consist of an electron-accepting 1,3,4-thiadiazole, 4-alkyl-1,2,4-triazole, or 3,4-dinitrothiophene unit and an electron-donating 1,4-didodecyloxybenzene or *N*-dodecylpyrrole unit, were prepared in 81−93% yields by palladium-catalyzed polycondensation. Their related model compounds (PhC≡C−Ar−C≡CPh; Ar = the electron-accepting unit) were also synthesized. GPC traces of the polymers gave number average molecular weights (M_n's) of 6900−29 700. The polymers formed a molecular assembly and a birefringent phase as revealed by powder X-ray diffraction (XRD) analysis and polarized light optical microscopy (POM). They formed an aligned structure on a platinum plate. The UV−vis peaks of the polymers appeared in the range of 385−522 nm in solutions, and the peak was shifted by 10−44 nm to a longer wavelength in films, according to intermolecular electronic interaction. The density functional theory (DFT) calculations supported the presence of strong intermolecular interaction between the polymer molecules. The polymers composed of a 1,3,4-thiadiazole or a 1,2,4-triazole unit exhibited photoluminescence with quantum yields of about 50% in chloroform. The polymers were electrochemically active and showed the reduction peak in a range of −1.1 through −2.2 V vs Ag^+/Ag.

Introduction

Among π-conjugated polymers, poly(aryleneethynylene)s (PAEs)[1] have attracted strong attention because of their interesting optical properties (e.g., photoluminescent property and optical nonlinearity),[2] rigid-rod molecular structure, and applications to sensors,[3] polarizers,[4] organic light-emitting diodes (OLEDs),[5] and molecular wires.[6] For PAEs, those having electron-deficient heteroaromatic rings such as pyridine,[2] 2,2′-bipyridyl,[7] 2,1,3-benzothiadiazole,[8] and quinoxaline[9] were recently prepared, and they showed interesting optical, electronic, and chemical properties.

The following five-membered 1,3,4-oxadiazole, 1,3,4-thiadiazole, and 4-alkyl-1,2,4-triazole with two electron-withdrawing imine (C=N) nitrogens possess a high electron affinity,[10] and PAEs consisting of these units are considered to be interesting.

Low-molecular-weight compounds of 1,3,4-oxadiazole and 4-phenyl-1,2,4-triazole are used as electron-transporting and hole-blocking materials to increase the quantum efficiency in OLEDs.[11] Recently, a large number of π-conjugated polymers containing the 1,3,4-oxadiazole unit have been synthesized and applied in OLEDs.[12] However, synthesis of PAEs bearing 1,3,4-thiadiazole and 1,2,4-triazole units in the conjugated main chain has not been reported. We herein report preparation of PAEs consisting of the 1,3,4-thiadiazole, 4-alkyl-1,2,4-triazole, and 3,4-dinitrothiophene units.

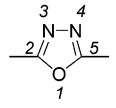

1,3,4-Oxadiazole

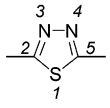

1,3,4-Thiadiazole

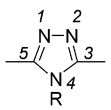

4-Alkyl-1,2,4-triazole

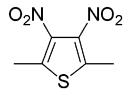

3,4-Dinitrothiophene

Recently, various alternative charge transfer (CT)-type π-conjugated copolymers (e.g., the following Polymer 1[13]) have been prepared and their interesting optical and electronic properties have been revealed.[13−16] The PAEs exhibited in Chart 1 have a similar CT structure, and are expected to show interesting chemical properties originated from the CT structure. Actually, we previously reported that PAEs containing electron-accepting units (e.g., diacetoxydicyano-*p*-phenylene unit in Polymer-2)[16] and electron-donating dialkoxy-*p*-phenylene unit had a strong tendency to form a molecular assembly because of the intermolecular CT interaction.

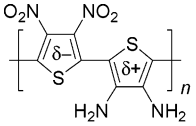

Polymer-1

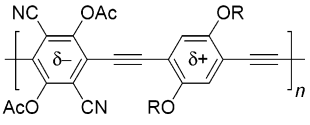

Polymer-2

The newly synthesized PAEs also contain electron-donating dialkoxy-*p*-phenylene or *N*-alkyl-2,5-pyrro-

* Author to whom correspondence should be addressed. E-mail: tyamamot@res.titech.ac.jp.
[†] Chemical Resources Laboratory.
[‡] Interdisciplinary Graduate School of Science and Engineering.

10.1021/ma050398p CCC: $30.25
Published on Web 04/23/2005

Chart 1

Newly synthesized PAEs

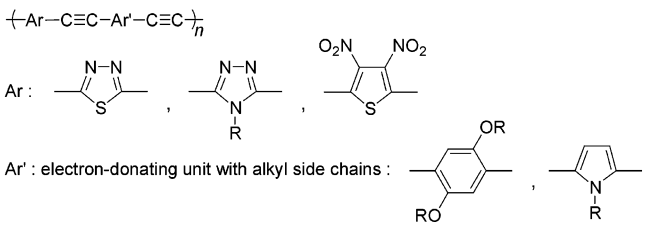

lylene unit and of the electron-accepting 1,3,4-thiadiazole, 4-alkyl-1,2,4-triazole, or 3,4-dinitrothiophene unit, and are expected to expand the scope of chemistry of PAEs with such a CT structure.

It has recently been reported that π-conjugated aromatic polymers with alkyl side chains (e.g., head-to-tail type regioregular poly(3-alkylthiophene)) tend to form a parallel alignment on the surface of substrates, with the alkyl side chain oriented toward the surface of the substrate.[8,17] Such alignment is considered to be crucial for higher carrier mobility[17b,c] and optical use[4a] of the π-conjugated aromatic polymer. However, the controlling factor for the alignment on the surface has not been clarified well, and the PAEs reported in this paper are expected to give experimental data for the controlling factors of such alignment on the surface of substrates.

To obtain further understanding of the electronic and optical properties of the newly prepared PAEs, we prepared the following trimeric model compounds consisting of the above-shown electron-accepting units. In the model compounds, the phenyl group is considered to behave as a donor unit, and the model compounds are also considered to have the CT electronic structure, Ph−C≡C−Ar−C≡C−Ph (Ar: the electron-accepting heteroaromatic unit).

Results and Discussion

New PAEs and Model Compounds. Scheme 1 exhibits synthetic routes of the polymers and model compounds. The dibromo monomers **1** through **3**[18] and the monomer **5**[8] were synthesized according to the literature. Details of synthesis of the new compounds **6**−**9** are described in the Experimental Section.

The new PAEs were prepared according to the polycondensation[1,19] under the Sonogashira−Heck coupling conditions,[20] and the results of the polymerization are summarized in Table 1. The polymerization proceeded smoothly at 60 °C to give the PAEs in high yields (81−93%). **P(Taz3-Ph)** and **P(Taz12-Ph)** were completely soluble in $CHCl_3$, THF, and 1,2-dichlorobenzene, and **P(Thdz-Ph)** was partially soluble (∼80%) in the solvents. **P(ThNO$_2$-Ph)** was less soluble in the solvents, and about 50% of the polymer was soluble in THF. **P(Thdz-Pyr**), **P(Taz12-Pyr)**, and **P(ThNO$_2$-Pyr)** with the *N*-dodecyl-2,5-pyrrolylene unit were soluble in the solvents; however, their solubility was somewhat lower compared with that of **P(Taz3-Ph)** and **P(Taz12-Ph)** having the didodecyloxy-*p*-phenylene unit. Thin films of the polymers suited for optical and electrochemical measurements were prepared by casting or spin coating.

GPC data of the soluble parts of PAEs indicated they had number average molecular weights (M_n's) of 6900−29 700 (vs polystyrene standards) with the polydispersity index (M_w/M_n) of 1.2−2.5. For **P(ThNO$_2$-Ph)**, the GPC analysis was carried out with the THF soluble part (about half, as described above), and the small M_w/M_n value of 1.2 (no. 4 in Table 1) was ascribed to the fractionation of **P(ThNO$_2$-Ph)** by the solubility.

PAEs usually have a −C−X (X = halogen) group at both polymer ends,[2c,21] suggesting that the reactivity of the dihalo monomer determine the molecular weight of the polymer. Of the dibromo monomers, **1** seems to have higher reactivity than **2** and **3**. For the polymers containing the 1,3,4-thiadiazole or 1,2,4-triazole unit, the M_n values (e.g., about 39 000 and 7500 for **P(Thdz-Ph)** and **P(Taz3-Ph)**, respectively) calculated from the Br content (see the Experimental Section) roughly agree with those obtained in the GPC analysis. However, the 3,4-dinitrothiophene-containing polymers show a large discrepancy between the M_n value estimated from the GPC analysis and that calculated from the Br content (e.g, M_n = about 52 000 for **P(ThNO$_2$-Ph)**, which may indicate that the polymer has a −C≡CH terminal group attributable to high reactivity of the monomer **4**.

Thermogravimetric analysis (TGA) exhibited that the 5% weight-loss temperature (T_d) of the copolymers was higher than 320 °C under N_2, except for **P(ThNO$_2$-Ph)** and **P(ThNO$_2$-Pyr)** with the nitro group (cf. Table 1 and Figure S2). The weight-loss of **P(ThNO$_2$-Ph)** and **P(ThNO$_2$-Pyr)** started around 200 °C, and the T_d's were 262 and 245 °C, respectively. The DSC curves of all the polymers exhibit an exothermicity at high temperatures (cf. Figure S3), suggesting occurrence of cross-linking that has been reported for PAE type polymers.[22] Once the polymer was heated above the high temperature, a different DSC curve was obtained.

IR and NMR. The IR spectra of all the polymers indicated a ν(C≡C) peak of the disubstituted acetylene in the range of 2181−2222 cm^{-1} (cf. Figure S1 in the Supporting Information), and the strong ν(C−H) peak (at 3286 cm^{-1} for **5** and at 3309 cm^{-1} for **6**) due to the terminal −C≡CH groups of the diethynyl monomer was not observed. **P(ThNO$_2$-Ph)** showed characteristic peaks of the $-NO_2$ group at 1552 and 1331 cm^{-1}.

As depicted in Figure 1, the ^{1}H NMR spectra of the polymers in $CDCl_3$ are reasonable for the molecular structures. **P(Thdz-Ph)**, **P(Taz3-Ph)**, and **P(ThNO$_2$-Ph)** give a single aromatic peak of the dialkoxy-*p*-phenylene unit at about δ 7.0−7.1, and peaks of the alkyl groups are observed in a normal region (δ 4.3−0.8). The aromatic signal of the pyrrole-based PAEs such as **P(Thdz-Pyr)** (Figure 1d) also appears at a normal position (at about δ 6.7). **P(ThNO$_2$-Pyr)** showed a weak paramagnetism in the temperature range of 4−300 K (cf. the Supporting Information; Figure S9). The magnetic susceptibility and ESR measurements of **P(ThNO$_2$-Pyr)** gave the spin concentration of approximately 0.1 spin/(repeating unit) at room temperature. NMR signals of **P(ThNO$_2$-Pyr)** could not be observed at room temperature because of the magnetism. **P(ThNO$_2$-Pyr)** exhibited some electrical conducting even at a nondoped state, as will be discussed later.

Molecular Structure, Molecular Assembly, and Morphology. We first determined molecular structures of the model compounds **7**−**9** by single-crystal X-ray crystallography, and the results are exhibited in Figures 2 and 3. The crystallographic data and refinement parameters are given in the Supporting Information (Table S1).

Molecular Structure of 7. Figure 2a displays a molecular structure of **7** in the crystal. **7** assumes a slightly twisted structure; the interplanar angles be-

Scheme 1. Syntheses of New PAEs and Model Compounds (C_nH_{2n+1} Indicates *n*-alkyl Group)

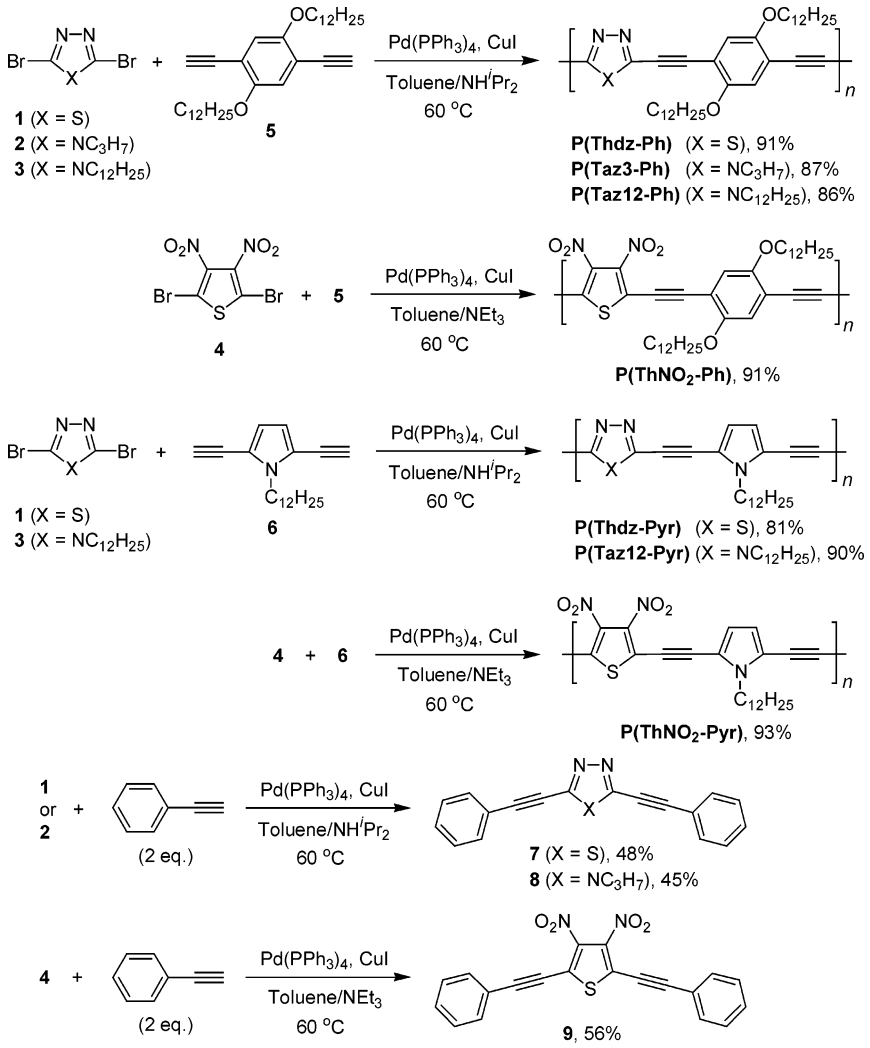

Table 1. Preparation of the PAEs[a]

no.	polymer	time (h)	yield (%)	color	M_n[b]	M_w/M_n[b]	T_d[d] (°C)
1	**P(Thdz-Ph)**	12	91	orange	29700	2.4	324
2	**P(Taz3-Ph)**	20	87	yellow	8200	2.0	357
3	**P(Taz12-Ph)**	20	86	yellow	17200	2.5	362
4	**P(ThNO$_2$-Ph)**	4	91	purple	7000[c]	1.2[c]	262
5	**P(Thdz-Pyr)**	24	81	red	19400	2.2	332
6	**P(Taz12-Pyr)**	40	90	brown	9700	1.8	370
7	**P(ThNO$_2$-Pyr)**	10	93	purple-black	6900[c]	1.4[c]	245

[a] The polymerization was carried out at 60 °C under N_2. [b] Estimated from GPC analysis for a $CHCl_3$ soluble part (eluent = $CHCl_3$; polystyrene standards), unless otherwise noted. [c] For a THF soluble part (eluent = THF; polystyrene standards). [d] 5% weight-loss temperature measured by TGA under N_2 with a heating rate of 10 °C min^{-1}.

tween the central 1,3,4-thiadiazole ring and the peripheral phenyl groups are ca. 9° and 15°. For ArC≡C−Ar′-C≡CAr type molecules, it has previously been reported that energy change with rotation of the aryrene units was very small;[23] however, in many cases, the molecule assumes essentially coplanar structure.[24] As seen in the crystal packing of **7** (Figure 2b), the short intermolecular contact distances, C2−C3′ (3.51 Å) and S1−N1′ (3.55 Å), indicate fairly strong intermolecular interactions between the neighboring two parallel molecules. In the case of **7**, the two molecules in the same column slipped by each other, and the 1,3,4-thiadiazole unit of the upper molecule comes approximately on the −C≡C− bond of the lower molecule. Similar slipped stacking of ArC≡C−Ar′-C≡CAr type molecules was reported.[24a,b] Because the two stacked molecules are not arranged in a completely parallel mode, it is difficult to determine the stacking distance. However, the stacking distance was roughly estimated at about 3.35 Å from the distance between C3′ and the thiophene ring in the lower molecule.

Structures of 8 and 9 with a Highly Polarized Central Ar Unit. On the other hand, the crystal packing of **8** and **9** (Figure 3) indicates a strong interaction between the central five-membered rings in the neighboring molecules. The stacking intermolecular distances in **8** and **9** are estimated at about 3.35 Å. Because the 4-propyl-1,2,4-triazole and 3,4-dinitrothiophene units are considered to have a very large electric dipole moment as discussed later, a strong antiparallel dipole−dipole interaction seems to control the molecular packing. The compound **8** assumes an

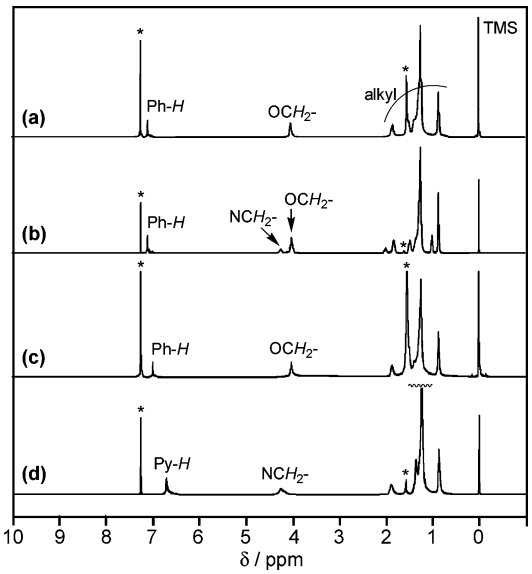

Figure 1. ^{1}H NMR spectra of (a) **P(Thdz-Ph)**, (b) **P(Taz3-Ph)**, (c) **P(ThNO$_2$-Ph)**, and (d) **P(Thdz-Pyr)** in $CDCl_3$. The peaks with * mark are due to $CHCl_3$ and H_2O.

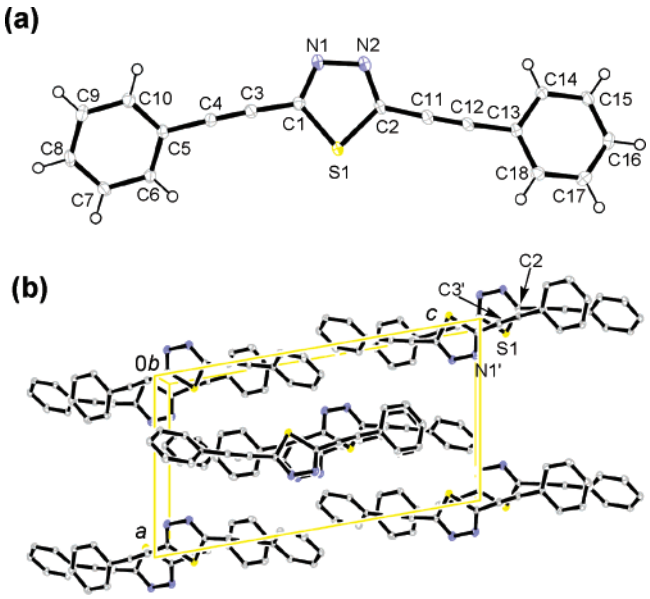

Figure 2. (a) ORTEP front view of **7**; selected bond lengths (Å) and angles (deg): S1−C1 1.732(1), N1−N2 1.364(2), N1−C1 1.316(1), C1−C3 1.418(2), C3−C4 1.202(2), C4−C5 1.432(2), C5−C6 1.402(2), C6−C7 1.388(2), C7−C8 1.391(2), C1−S1−C2 86.65(6), N2−N1−C1 112.4(1), S1−C1−N1 114.13(9), N1−C1−C3 124.2(1), C1−C3−C4 176.8(1), C3−C4−C5 178.2(1), C4−C5−C6 119.5(1), C5−C6−C7 120.1(1). (b) Packing view of **7** along the *b* axis. Hydrogen atoms are omitted for simplification.

essentially coplanar structure; however, **9** takes a somewhat twisted structure with an interplanar angle of ∼25°. This is considered to be due to the electronic and steric effects of the NO_2 group, and DFT calculation (B3LYP/6-31G*) also predicted a twisted structure of **9** with the interplanar angle of about 7°. The two NO_2 groups are not in the same plane of thiophene because of steric reason.

Packing Structure of PAEs with a Dialkoxy-*p*-phenylene Unit. For the PAEs with the dialkoxy-*p*-phenylene unit, the packing structure shown in Figure 4, which is similar to that proposed for a similar CT-type PAE,[8] is supposed on the basis of XRD data described below.

We assume an idealized packing structure for PAEs, in which the stiff conjugated main chains form essentially a coplanar structure and the alkoxy side chains are extended laterally within the planes of the main chains. Appropriate arrangement of the directions of the dipoles located on the five-membered heterocycles is considered to play an important role in formation of a layered π-stacked assembly.[25] Side chain crystallization (or aggregation) is also considered to be an important role in the formation of the assembly.[17,26−28]

As illustrated in Figure 4, the polymer molecules in a layer are considered to take a zigzag conformation and an interdigitation[27] packing mode. The repeating height, h = ∼13 Å (cf. Figure 4), of the polymer is larger than the double of the effective thickness of the alkoxy side chain[8,27] (about 4.5 Å) to allow the interdigitation packing.

The powder X-ray diffraction (XRD) pattern of **P(Thdz-Ph)** gives three diffraction peaks at d_1 = 21.3 Å, d_2 = 4.3 Å, and d_3 = 3.5 Å, as exhibited in Figure 5a. The sharp d_1 peak can be assigned to a distance between the conjugated main chains separated by the long side chains (cf. Figure 4); similar assignment has been made for various π-conjugated polymers with long side chains.[17]

Poly((2,5-didodecyloxy-*p*-phenylene)ethynylene), having a higher concentration of the same $-OC_{12}H_{25}$ side chains, was reported to take a lamellar structure in the solid and gave a longer interchain distance of d = 29.5 Å,[21b] which suggests formation of a somewhat different packing mode (presumably an end-to-end packing mode[17,26,27]) because of the dense $-OC_{12}H_{25}$ chains. The d_3 peak of 3.5 Å observed with **P(Thdz-Ph)** (Figure 5a) is reasonable for the layer-to-layer π-stacking distance (cf. Figure 4) between the coplanar polymer molecules, as previously reported for coplanar π-conjugated poly(heteroarylene)s such as head-to-tail poly(3-alkylthiophene)s and head-to-head poly(4-alkylthiazole)s.[17,26] The d_3 distance of **P(Thdz-Ph)** is comparable to that of the intermolecular stacking distance (about 3.4 Å) of **7** discussed above. The d_2 peak corresponds to a side-to-side distance between loosely packed alkyl side chains.[27]

The XRD patterns shown in Figures 5b and 5d suggest that **P(Taz3-Ph)** and **P(ThNO$_2$-Ph)** assume a similar self-assembled layered structure in the solid. The packing model, the d_1 and d_3 values, and the repeating height (cf. Figure 4; h = ∼13 Å) give calculated densities of 0.99, 0.99, and 1.10 g cm^{-3} for **P(Thdz-Ph)**, **P(Taz3-Ph)**, and **P(ThNO$_2$-Ph)**, respectively. These calculated densities (ρ_s) essentially agree with the observed densities of 0.95, 0.97, and 1.05 g cm^{-3} within experimental error, supporting the proposed packing structure; the observed ρ value is usually smaller than the calculated value because polymers usually contain an amorphous part.

P(Taz12-Ph) has a larger number density of the long side chain and may assume a somewhat different packing mode in the solid. If **P(Taz12-Ph)** assumes a similar packing structure, the d_3 peak is considered to be hidden under the d_2 peak. The d_1 distance does not show a strong dependence on the presence or absence of the alkyl side chain in the 1,3,4-thiadiazole and 1,2,4-triazole units, revealing that the distance d_1 between the π-conjugated main chains is essentially determined by the two dodecyloxy side chains of the didodecyloxy-*p*-phenylene unit. However, the d_1 distance somewhat increases with the increase in the length of the alkyl side chain (from 21.3 Å of **P(Thdz-Ph)** to 26.8 Å of

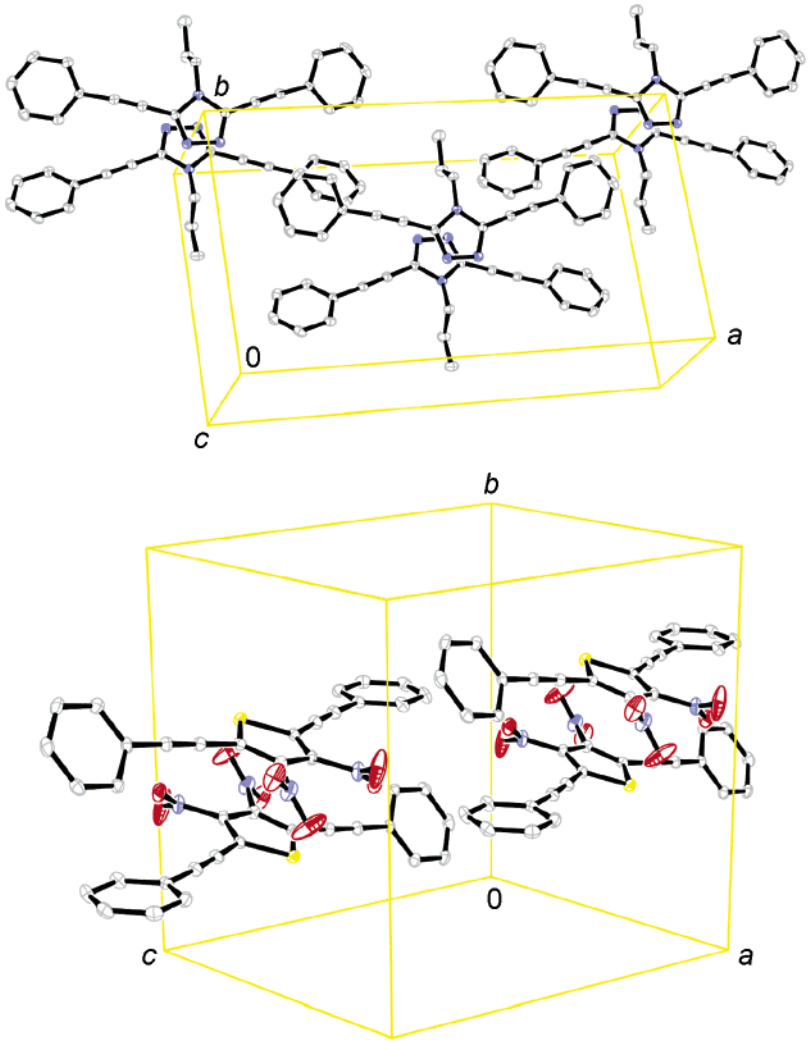

Figure 3. Molecular packing of **8** (top) and **9** (bottom). Hydrogen atoms are omitted for simplification.

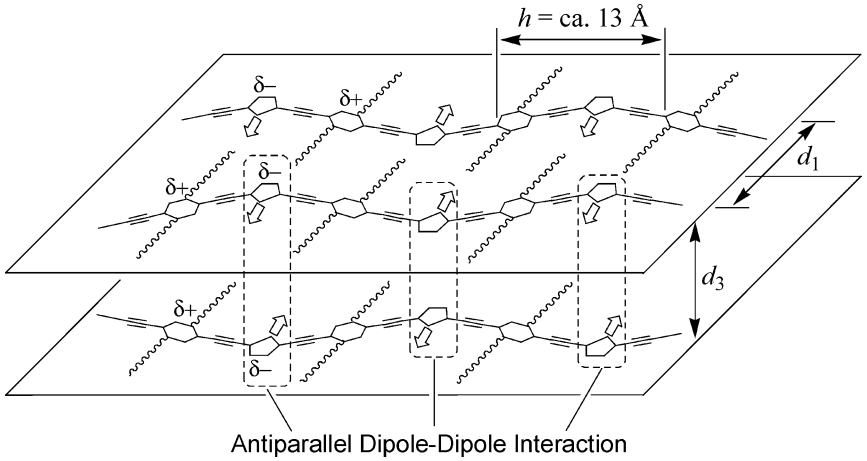

Figure 4. Schematic representation of a proposed packing structure of the polymers in the solid state. The arrows indicate directions of the dipole moment on the five-membered heterocycles. The polymer with long side chains assumes an interdigitation packing mode, and segregation of the polymer main chains accounts for the interchain d_1 spacing. The repeating height, h, is estimated at 13.0 Å for **P(Thdz-Ph)**, 12.6 Å for **P(Taz3-Ph)**, and 13.1 Å for **P(ThNO$_2$-Ph)**.

P(Taz12-Ph), cf. Figure 5) presumably due to increase of the volume to be allotted for the alkyl and dodecyloxy side chains.

Polarized light optical microscopy (POM) showed a birefringent phase in a thin film of **P(Thdz-Ph)** at room temperature, as displayed in Figure 6, and the phase was unchanged at 180 °C. Phase transition to an isotropic phase could not be detected because the sample decomposed before reaching the isotropic phase. The polarized microscopy and DSC traces revealed that the endothermic peaks of **P(Taz3-Ph)** and **P(Taz12-Ph)** at 81 °C and 171 °C, respectively, corresponded to transition to an isotropic phase. Films of the pyrrole-based polymers did not show an optically anisotropic phase.

Packing Structure of PAEs with a *N*-dodecyl-2,5-pyrrolylene Unit. In contrast to the case of PAEs with

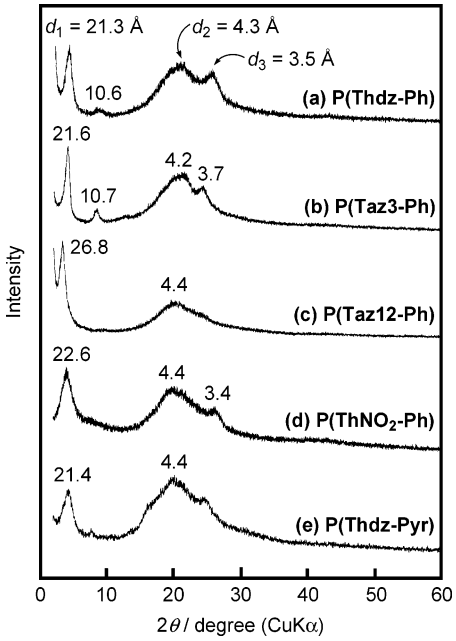

Figure 5. Powder X-ray diffractograms of (a) **P(Thdz-Ph)**, (b) **P(Taz3-Ph)**, (c) **P(Taz12-Ph)**, (d) **P(ThNO$_2$-Ph)**, and (e) **P(Thdz-Pyr)**. Peaks are labeled with d-spacing in angstroms. The peaks at $2\theta = 8.3°$ ($d = 10.6$ Å) of **P(Thdz-Ph)** and $2\theta = 8.2°$ ($d = 10.7$ Å) of **P(Taz3-Ph)** are assigned to (020) peaks with spacing of $d_1/2$.

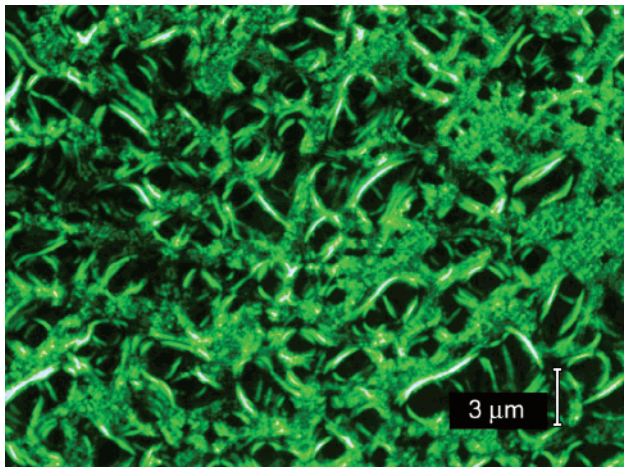

Figure 6. Polarized microscopic image of a cast film of **P(Thdz-Ph)** under crossed polarizers at room temperature.

the symmetrical didodecyloxy-*p*-phenylene unit, well-packing of PAEs with the unsymmetrical *N*-dodecyl-2,5-pyrrolylene unit requires additional ordering of the direction of the alkyl group of the *N*-dodecyl-2,5-pyrrolylene unit. Consequently, it may be difficult for these polymers with the *N*-dodecyl-2,5-pyrrolylene unit to form a well-packed structure. The somewhat broad peak of **P(Thdz-Pyr)** shown in Figure 5e may indicate the difficulty for these polymers to form the well-packed structure, and the following data concerning molecular alignment on the surface of platinum plate support this view.

Molecular Alignment on the Surface of a Pt Plate. Figure 7 exhibits XRD patterns of cast films of the PAEs on a Pt plate. As seen from Figure 7, the XRD patterns of the cast films of **P(Thdz-Ph)**, **P(Taz3-Ph)**, and **P(ThNO$_2$-Ph)** clearly show the d_1 (cf. Figures 4 and 5) peak; however, the d_2 and d_3 peaks observed in Figure 5 almost vanish. The d_1 distance is somewhat

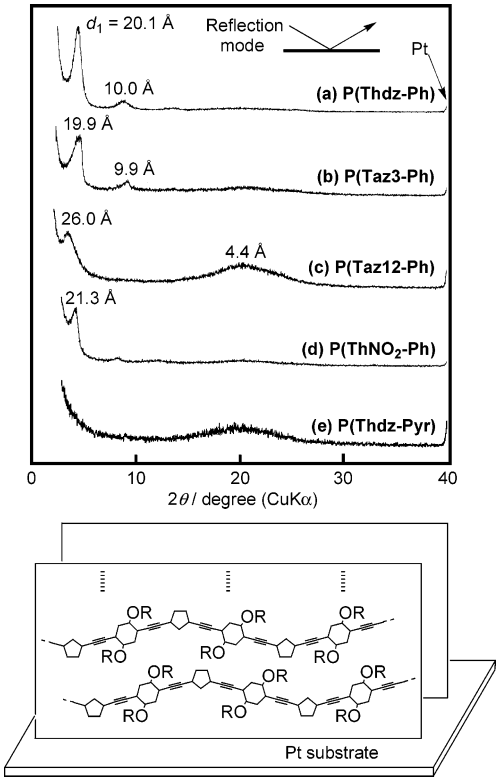

Figure 7. Top: XRD patterns of cast films of (a) **P(Thdz-Ph)**, (b) **P(Taz3-Ph)**, (c) **P(Taz12-Ph)**, (d) **P(ThNO$_2$-Ph)**, and (e) **P(Thdz-Pyr)** on a Pt substrate. The XRD patterns were obtained with a reflection mode. Bottom: Alignment of PAE molecules on a Pt substrate.

shortened and the second-order $d_1/2$ peak is observed for **P(Thdz-Ph)** and **P(Taz3-Ph)**, similar to the cases of Figures 5a and 5b. As previously reported, with π-conjugated polymers with long alkyl side chains,[8,17] the disappearance of the d_2 and d_3 peaks of **P(Thdz-Ph)**, **P(Taz3-Ph)**, and **P(ThNO$_2$-Ph)** in the XRD patterns of their cast films is considered to indicate parallel alignment of these PAE molecules on the surface of the Pt plate, which is depicted in the bottom of Figure 7. The present results give new examples of such alignment of the π-conjugated aromatic polymers and suggest that the CT-type PAE with long side chains has a tendency to take such an aligned structure on the surface of substrates. It was previously reported that π-conjugated polymers such as head-to-tail type poly(3-alkylthiophene-2,5-diyl) with long alkyl side chains form an aligned structure on the surface of various substrates such as Pt plate, Si plate, glass plate, and Teflon plate.[8d,17] The polymers described above are also expected to form a similar aligned structure on various substrates, too. However, the XRD pattern of **P(Taz12-Ph)** exhibits the d_2 peak as shown in Figure 7c, revealing that this polymer does not form such an aligned structure. The too long $-C_{12}H_{25}$ side chain may prevent formation of such an ordered structure during the formation of the cast film. For **P(Thdz-Pyr)** with the *N*-dodecyl-2,5-pyrrolylene unit, the polymer seems to form an amorphous cast film as shown in Figure 7e, presumably due to the difficulty in forming the ordered structure discussed above.

UV−vis and Photoluminescence (PL) Data. The UV−vis and photoluminescence (PL) spectra of the polymers in solutions are depicted in Figure 8. Optical data of the polymers in solutions and films are sum-

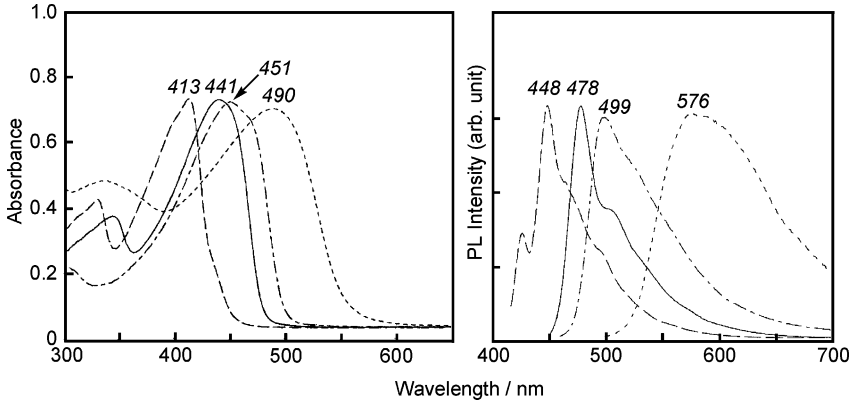

Figure 8. UV−vis absorption (left) and PL (right) spectra of **P(Thdz-Ph)** (——), **P(Taz3-Ph)** (- - -), **P(Thdz-Pyr)** (- • - • -) in $CHCl_3$, and **P(ThNO$_2$-Ph)** (• • •) in THF at room temperature. The PL spectra were obtained under excitation with λ_{max} light.

Table 2. Optical and Electrochemical Data of the PAEs and the Model Compounds[a]

		UV−vis absorption			photoluminescence			
no.	compound	λ_{max} in solution (nm)	log ϵ[c]	λ_{max} in film (nm)	λ_{em} in solution (nm)	Φ[f] (%)	λ_{em} in film (nm)	reduction peak potential[g] (V vs Ag^+/Ag)
1	**P(Thdz-Ph)**	441	4.46	485	478	52	560	−1.83
2	**P(Taz3-Ph)**	413	4.58	436	448	57	521 (495)	−1.98
3	**P(Taz12-Ph)**	412	4.59	425	449 (465)	46	540	−1.99
4	**P(ThNO$_2$-Ph)**	490[b]	4.38[b]	506	576[b]	3[b]	*e*	−1.18, −1.43
5	**P(Thdz-Pyr)**	451	*d*	484	499	45	587	−1.84
6	**P(Taz12-Pyr)**	385	*d*	395	415 (438)	5	526	−2.20
7	**P(ThNO$_2$-Pyr)**	522[b]	*d*	538	*e*	*e*	*e*	−1.37, −1.88
8	**7**	334	4.56		396	15		*d*
9	**8**	299	4.60		352 (337,365)	16		*d*
10	**9**	382	4.39		508	0.4		*d*

[a] With the $CHCl_3$ soluble part and in $CHCl_3$, unless otherwise noted. The data in parentheses are due to subpeaks. [b] With the THF soluble part and in THF. [c] Molar extinction coefficient based on the repeating unit. [d] Not determined. [e] Too weak to measure. [f] PL quantum yield calculated by using the standard of quinine sulfate (10^{-5} M solution in 0.5 M H_2SO_4) having Φ of 54.6%. [g] Estimated from cyclic voltammetry for cast films.

marized in Table 2. **P(Taz3-Ph)** gives an absorption maximum (λ_{max}) at 413 nm in $CHCl_3$; the λ_{max} position is located near the $\pi-\pi^*$ transition peak reported for poly((2,5-dialkoxy-*p*-phenylene)ethynylene)s (λ_{max} = ∼400−430 nm in solutions).[21,28]

The λ_{max}s of **P(Thdz-Ph)** and **P(ThNO$_2$-Ph)** are observed at a considerably longer wavelength (λ_{max} = 441 nm in $CHCl_3$ and 490 nm in THF, respectively). Incorporation of the 3,4-dinitrothiophene unit into the polymer main chain leads to a bathochromic shift of the absorption peak, which is ascribed to the enhanced intramolecular CT structure in **P(ThNO$_2$-Ph)** (vide infra). The longer λ_{max} value of **P(Thdz-Ph)** than that of **P(Taz3-Ph)** may also account for enhancement of the contribution from the CT electronic structure because the difference between S in the 1,3,4-thiadiazole unit and N in the 1,2,4-triazole unit will render a larger electron affinity to the 1,3,4-thiadiazole unit, similar to cases of thiophene and pyrrole. In films, the λ_{max} positions are shifted to a longer wavelength because of the discussed molecular stacking in the solid.

The copolymers with the *N*-dodecyl-2,5-pyrrolylene unit show a similar effect of the dinitrothiophene unit, and the $\pi-\pi^*$ transition energy decreases in the order of **P(Taz12-Pyr)** (λ_{max} = 385 nm) > **P(Thdz-Pyr)** (λ_{max} = 451 nm) > **P(ThNO$_2$-Pyr)** (λ_{max} = 522 nm) in their solutions (cf. Table 2). For **P(Taz12-Pyr)**, the long alkyl side chains in the 1,2,4-triazole unit and pyrrole unit may cause some steric repulsion between them to distort the coplanarity of the main chain, and this effect may also contribute to a shift of λ_{max} to a relatively shorter wavelength. Such an effect of the long alkyl side chain is also observed in the electrochemical behavior of **P(Taz12-Pyr)**, as discussed below.

P(Taz3-Ph), **P(Thdz-Ph)**, and **P(Thdz-Pyr)** in $CHCl_3$ exhibited intense light-blue, green, and yellow-green PL emissions with the peaks at 448, 478, and 499 nm (Figure 8, right), respectively, when irradiated with their λ_{max} light. Some of the PAEs gave the quantum yield (Φ) higher than 50%. The PL peak (λ_{em}) positions of these polymers roughly agreed with the onset position of the absorption band, as usually observed with π-conjugated polymers. As seen from Table 2, the λ_{em} position is shifted by about 70−110 nm toward a longer wavelength in film, with broadening of the peak. Such a shift in the solid is often observed with π-conjugated polymers and assigned to formation of an excimer-like adduct.[1,29] The nitro-substituted **P(ThNO$_2$-Ph)**, **P(ThNO$_2$-Pyr)**, and **9** showed only a very weak PL; it is known that a nitro group often brings about such a diminishing effect on PL.

Electronic State of the Model Compounds 7−9. Figure 9 displays the frontier orbital distribution in structurally optimized **7**−**9**; the calculation is made at a B3LYP/6-31G* level. Results for their alkoxy-substituted derivatives are given in the Supporting Information (Figure S6). HOMO and LUMO of **7** and **8** are expanded over the whole of the molecule. In contrast, the LUMO of **9** (see Figure 9c) is somewhat localized on the 3,4-dinitrothiophene moiety, especially on the nitro groups. From the results, it is deduced that the HOMO−LUMO $\pi-\pi^*$ transition in **9** is accompanied by a strong intramolecular CT from the donor to the acceptor parts. Calculated HOMO−LUMO $\pi-\pi^*$ transi-

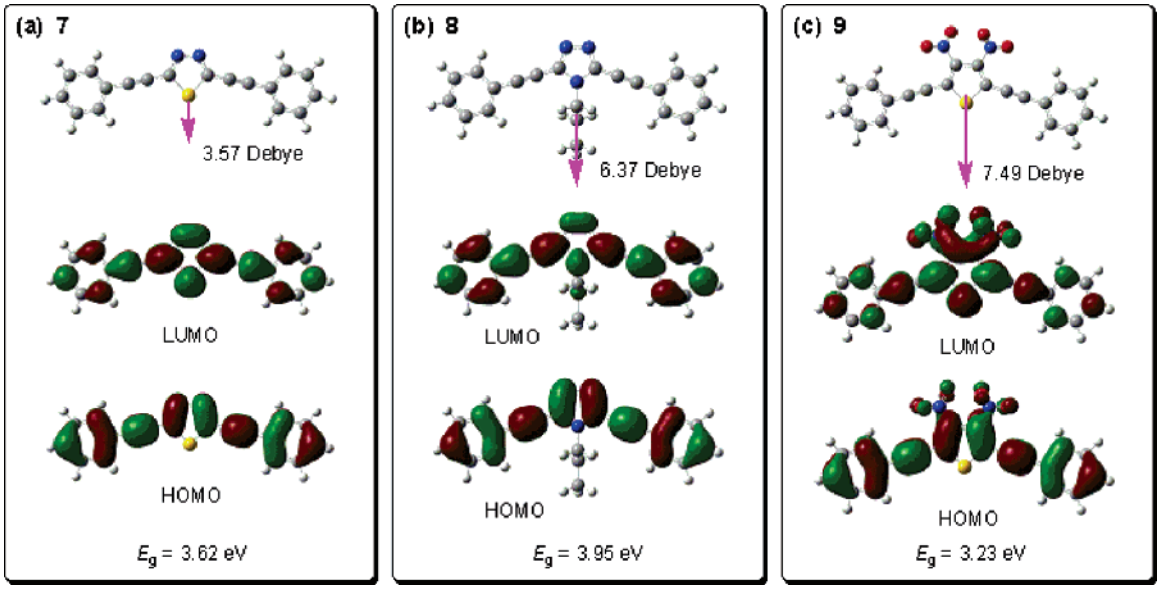

Figure 9. The highest occupied molecular orbital (HOMO) and the lowest unoccupied molecular orbital (LUMO) for the optimized geometry of **7**−**9** calculated at the B3LYP/6-31G* level. Arrows indicate the dipole moment of the molecules.

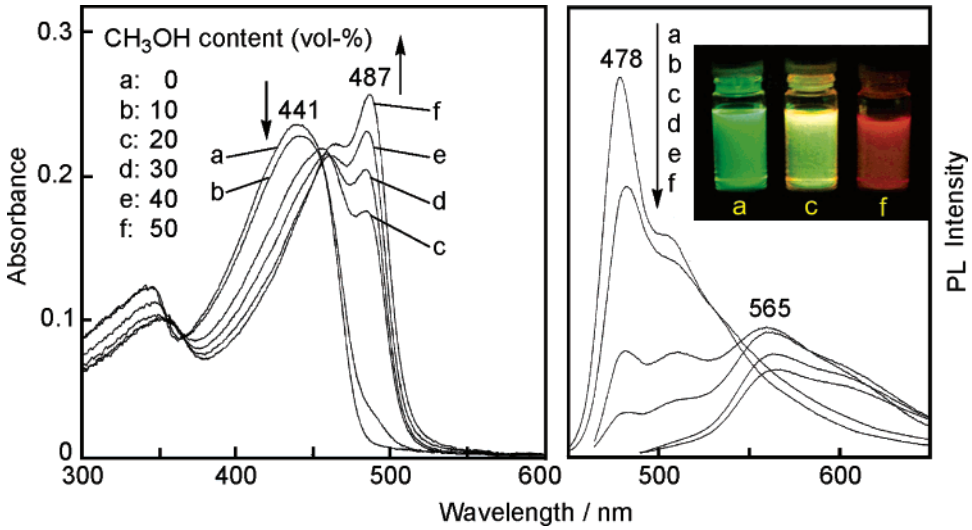

Figure 10. Changes in UV−vis (left) and PL (right) spectra of $CHCl_3$ solution of **P(Thdz-Ph)** on addition of CH_3OH (0−50 vol %). Arrows indicate the direction of the spectral change from low to high CH_3OH content. The inset in the PL spectra displays a photograph showing emission of light from the polymer solution, depending on the CH_3OH content. [**P(Thdz-Ph)**] = 8.0×10^{-6} M (repeating unit).

tion energy decreases in agreement with the observed sequence of **8** (E_g = 3.95 eV) > **7** (3.62 eV) > **9** (3.23 eV), although the calculated E_g values of **7**−**9** are somewhat (~0.3−0.5 eV) larger than the optical energy gap estimated from the onset position of their UV−vis spectra.

Self-assembly in Solution. As discussed above, the synthesized PAEs have a strong tendency to stack, and this stacking can also be observed with solution systems. Figure 10 exhibits changes in the UV−vis and PL spectra of a $CHCl_3$ solution of **P(Thdz-Ph)**, which is caused by addition of CH_3OH, a poor solvent for **P(Thdz-Ph)**. When CH_3OH is added, a new absorption peak appears at 487 nm. The new absorption peak agrees with the λ_{max} position of the film of **P(Thdz-Ph)**, suggesting that colloidal particles are formed by addition of CH_3OH; in the colloidal particle, the polymer molecules are considered to assume a stacking structure similar to that in the film. Filtration of the colloidal solution[26] decreased the absorbance at 487 nm, and data obtained by filtration of the solution with membranes with various pore sizes revealed that the colloidal solution containing 20 vol % of CH_3OH (curve c in Figure 10) contained 14% of colloidal particles larger than 0.20 μm, 19% of those with 0.20−0.10 μm size, 48% of those with 0.1−0.02 μm size, and 19% of those less than 0.02 μm. Other copolymers exhibited analogous solvatochromism; e.g., the data for **P(Taz3-Ph)** are shown in the Supporting Information (Figure S7).

As presented in the right part of Figure 10, addition of CH_3OH to the $CHCl_3$ solution of **P(Thdz-Ph)** leads to a large red-shift of the PL peak and a decrease in the PL intensity. Dramatic color changes of the emitted lights from green to orange are observed on addition of CH_3OH. As shown in Table 2 (no. 1), the PL peak of **P(Thdz-Ph)** in $CHCl_3$ at 478 nm shifts to 560 nm in film, and a similar shift is observed with the solution

containing a large amount of CH_3OH (more than 40 vol %).

Electrochemical Properties. The redox properties of the polymers were characterized by cyclic voltammetry (CV) with their cast films, and the results are shown in Table 2 and the Supporting Information (Figure S8). The electrochemical reduction of **P(Thdz-Ph)** started at about −1.6 V and gave an irreversible cathodic peak at −1.83 V vs Ag^+/Ag. This reduction onset potential is comparable to that of typical electron-transporting polymers such as cyano-substituted poly(*p*-phenylenevinylene), CN−PPV (−1.6 V vs Ag^+/Ag),[30a] and 1,3,4-oxadiazole-containing aromatic polymers (ca. −1.5 to −1.8 V vs Ag^+/Ag).[30b−d] According to the reduction, the color of the film of **P(Thdz-Ph)** changed from orange under a neutral state to black under a reduced state. When swept anodically, an irreversible oxidation peak at 1.33 V vs Ag^+/Ag was obtained, which is mainly associated with oxidation of the dialkoxy-*p*-phenylene unit.

Reduction of **P(Taz3-Ph)** required a negatively higher potential (−1.98 V vs Ag^+/Ag) than that of **P(Thdz-Ph),** reflecting lower electron-accepting properties of the 1,2,4-triazole unit discussed above. For **P($ThNO_2$-Ph)**, the reductive scan gave two cathodic peaks at −1.18 and −1.43 V vs Ag^+/Ag; it has been reported that various aromatic compounds with the nitro group show similar two-step reduction.[31] The difference in the reduction potential among the polymers may be explained by the difference of intramolecular CT characteristics.

P(Thdz-Ph), **P(Taz3-Ph)**, and **P(Taz12-Ph)** themselves were insulating materials with electrical conductivity less than 10^{-11} S cm^{-1}; however, **P($ThNO_2$-Ph)** and **P($ThNO_2$-Pyr)** having the 3,4-dinitrothiophene unit exhibited electrical conductivity of 9.7×10^{-9} and 6.3×10^{-9} S cm^{-1}, respectively, even at a nondoped state as discussed above. It has been reported that several π-conjugated polymers with a nitro group such as poly(4,8-dinitroanthraquinone-1,5-diyl) show unique magnetism and electrical conductivity;[32] contribution of resonance structures participated in by the nitro group may generate a carrier in the polymer main chain. **P($ThNO_2$-Pyr)** indicated weak paramagnetism as described above.

Conclusions

New poly(aryleneethynylene)s (PAEs) and their model compounds consisting of electron-accepting 1,3,4-thiadiazole, 1,2,4-triazole, and 3,4-dinitrothiophene units were prepared. Most of PAEs formed a self-assembled π-stacked structure in the solid assisted by the antiparallel dipole−dipole interaction and side chain aggregation, as revealed by X-ray analyses and polarized optical microscopy. They showed a strong tendency to be aligned on a Pt plate. UV−vis and PL properties of PAEs in chloroform changed upon addition of methanol because of formation of colloidal aggregates. Quantum-chemical calculations of the model compounds support the intramolecular CT structure of PAEs. The synthesized PAEs were photoluminescent, and some PAEs gave the quantum yield of about 50%. They were electrochemically active.

Experimental Section

Materials and Syntheses. 2,5-Dibromo-1,3,4-thiadiazole (**1**),[18] 3,5-dibromo-4-propyl-1,2,4-triazole (**2**),[18] 3,5-dibromo-4-dodecyl-1,2,4-triazole (**3**),[18] 1,4-didodecyloxy-2,5-diethynylbenzene (**5**),[28] 2,5-dibromo-*N*-dodecylpyrrole,[33] and $Pd(PPh_3)_4$[34] were prepared by similar procedures reported in the literature. Commercially available 2,5-dibromo-3,4-dinitorothiophene (**4**) was used for the polymerization. Solvents (anhydrous grade) used in the reactions were purchased from Aldrich Co. or Kanto Chemical Co. and stored under an inert atmosphere.

2,5-Diethynyl-*N*-dodecylpyrrole (6). 2,5-Dibromo-*N*-dodecylpyrrole (9.83 g, 25 mmol), $Pd(PPh_3)_4$ (1.16 g, 1.0 mmol), and CuI (0.19 g, 1.0 mmol) were mixed with dry THF (40 mL) and triethylamine (40 mL) under N_2. Trimethylsilyl acetylene (5.89 g, 60 mmol) was slowly added to the mixture at room temperature. The reaction mixture was stirred for 12 h at 50 °C, and then the solvent was removed by evaporation. The residue was dissolved in hexane, and the solution was passed through a short column of Celite to eliminate the ammonium salt. The obtained product was further passed through a short column (silica, hexane/chloroform = 3:1, v/v). Evaporation of the solvent led to a yellow oil of the silylated intermediate. This material was dissolved in a mixture of THF (30 mL) and methanol (100 mL). An aqueous solution of potassium hydroxide (1.0 M, 20 mL) was added to the solution, and the mixture was stirred for 10 h at room temperature. It was then poured into water, and the product was extracted three times with hexane. The combined extracts were washed with water and dried over anhydrous sodium sulfate. After filtration and evaporation, the product was further purified with column chromatography (silica, hexane/chloroform = 9:1, v/v) and dried under vacuum to give a light-yellow oil (yield = 5.38 g, 76%). ^1H NMR (400 MHz, $CDCl_3$): δ 6.37 (s, 2H), 4.07 (t, 7.4 Hz, 2H), 3.33 (s, 2H, acetylenic-*H*), 1.77 (m, 2H), 1.30−1.25 (m, 18H), 0.88 (t, 6.8 Hz, 3H). $^{13}C\{^1H\}$ NMR (100 MHz, $CDCl_3$): δ 115.56, 114.95, 81.43, 75.44, 46.45, 31.97, 30.77, 29.71, 29.68, 29.64, 29.54, 29.39, 29.24, 26.56, 22.75, 14.19. FT-IR (neat, cm^{-1}): 3309, 2925, 2854, 2104, 1464, 1405, 1375, 1318, 1131, 1024, 768. Anal. Calcd for $C_{20}H_{29}N$: C, 84.75; H, 10.31; N, 4.94. Found: C, 84.49; H, 10.04; N, 5.07.

P(Thdz-Ph). To a solution of **1** (488 mg, 2.0 mmol) and **5** (990 mg, 2.0 mmol) in dry toluene (70 mL) were added dry diisopropylamine (30 mL), $Pd(PPh_3)_4$ (120 mg, 0.1 mmol), and CuI (20 mg, 0.1 mmol) under N_2. The mixture was stirred for 0.5 h at room temperature and for 12 h at 60 °C. After cooling to room temperature, the solvent was removed under reduced pressure. The resulting residue was dissolved in chloroform, and the solution was slowly added into methanol to obtain a precipitate. The crude product was separated by filtration and washed with acetone. The crude polymer was further dissolved in chloroform and reprecipitated in methanol. **P(Thdz-Ph)** was collected by filtration, dried under vacuum, and obtained as an orange solid (yield = 1.05 g, 91%). ^1H NMR (400 MHz, $CDCl_3$): δ 7.11 (s, 2H), 4.04 (br, 4H), 1.86 (br, 4H), 1.52−1.24 (br, 36H), 0.86 (br, 6H). FT-IR (KBr, cm^{-1}): 2924, 2852, 2212, 1505, 1469, 1439, 1379, 1278, 1219, 1109, 1022, 858, 718. Anal. Calcd for Br−$(C_{36}H_{52}N_2O_2S)_{67}$−$C_2N_2SBr$ (M_n = 38 896): C, 74.54; H, 9.03; N, 4.90; O, 5.51; S, 5.61; Br, 0.41. Found: C, 74.83; H, 8.93; N, 4.68; O, 5.79; S, 5.69; Br, 0.41.

Other PAEs were prepared analogously. The spectroscopic and analytical data of the polymers are described below. Some of PAEs are considered to be hydrated.

P(Taz3-Ph). Yellow solid (yield = 87%). ^1H NMR (400 MHz, $CDCl_3$): δ 7.12 (s, 2H), 4.26 (br, 2H), 4.03 (br, 4H), 2.00 (br, 2H), 1.84 (br, 4H), 1.49−1.25 (m, 36H), 1.01 (t, 3H), 0.87 (t, 6H). FT-IR (KBr, cm^{-1}): 2924, 2853, 2222, 1736, 1521, 1466, 1387, 1278, 1221, 1025, 860, 718. Anal. Calcd for Br−$(C_{39}H_{59}N_3O_2)_{12}$−$C_5H_7N_3Br$ (M_n = 7492): C, 75.83; H, 9.62; N, 7.29; O, 5.12; Br, 2.13. Found: C, 75.87; H, 9.42; N, 6.64; O, 5.99; Br, 2.12.

P(Taz12-Ph). Yellow solid (yield = 86%). ^1H NMR (400 MHz, $CDCl_3$): δ 7.12 (s, 2H), 4.27 (br, 2H), 4.03 (br, 4H), 1.95 (br, 2H), 1.84 (br, 4H), 1.49−1.20 (m, 54H), 0.88−0.84 (m, 9H). FT-IR (KBr, cm^{-1}): 2924, 2852, 2222, 1739, 1521, 1467, 1387, 1278, 1220, 1022, 860, 720. Anal. Calcd for Br−$(C_{48}H_{77}N_3O_2 \cdot 0.4H_2O)_{40}$−$C_{14}H_{25}N_3Br$ (M_n = 29 809): C, 77.92; H, 10.61; N, 5.78; O, 5.15; Br, 0.54. Found: C, 77.46; H, 10.58; N, 5.63; O, 5.31; Br, 0.53.

P(ThNO$_2$-Ph). Triethylamine was used for the polymerization, instead of diisopropylamine. Purple powder (yield = 91%). ^{1}H NMR (400 MHz, $CDCl_3$): δ 7.00 (s, 2H), 4.03 (br, 4H), 1.88 (br, 4H), 1.55−1.24 (m, 36H), 0.86 (br, 6H). FT-IR (KBr, cm^{-1}): 2924, 2852, 2199, 1630, 1552, 1466, 1389, 1331, 1281, 1220, 1129, 1018, 862, 721. Anal. Calcd for $(C_{38}H_{52}N_2O_6S)_n$: C, 68.64; H, 7.88; N, 4.21; O, 14.44; S, 4.82. Found: C, 68.44; H, 7.82; N, 3.82; O, 14.48; S, 4.43; Br, 0.31.

P(Thdz-Pyr). Red solid (yield = 81%). ^{1}H NMR (400 MHz, $CDCl_3$): δ 6.71 (s, 2H), 4.26 (br, 2H), 1.88 (br, 2H), 1.35−1.22 (m, 18H), 0.86 (br, 3H). FT-IR (KBr, cm^{-1}): 2923, 2851, 2197, 1457, 1389, 1321, 1197, 1119, 1027, 767, 733. Anal. Calcd for Br−$(C_{22}H_{27}N_3S\cdot 0.1H_2O)_{70}$−$C_2N_2SBr$ (M_n = 25 957): C, 71.34; H, 7.39; N, 11.44; O, 0.43; S, 8.77; Br, 0.62. Found: C, 71.43; H, 7.46; N, 10.89; O, 0.28; S, 8.21; Br, 0.61.

P(Taz12-Pyr). Brown solid (yield = 90%). ^{1}H NMR (400 MHz, $CDCl_3$): δ 6.64 (br, 2H), 4.16 (br, 4H), 1.88 (br, 4H), 1.24 (br, 36H), 0.87 (br, 6H). FT-IR (KBr, cm^{-1}): 2924, 2853, 2213, 1740, 1466, 1416, 1397, 1028, 767, 720. Anal. Calcd for Br−$(C_{34}H_{52}N_4\cdot 0.4H_2O)_{29}$−$C_{14}H_{24}N_3Br$ (M_n = 15 590): C, 77.04; H, 10.05; N, 10.69; O, 1.19; Br, 1.03. Found: C, 76.37; H, 9.81; N, 10.12; O, 1.13; Br, 1.00.

P(ThNO$_2$-Pyr). Triethylamine was used for the polymerization instead of diisopropylamine. Purple-black powder (yield = 93%). FT-IR (KBr, cm^{-1}): 2923, 2852, 2181, 1609, 1522, 1457, 1376, 1308, 1234, 1130, 771. Anal. Calcd for $(C_{24}H_{27}N_3O_4S)_n$: C, 63.56; H, 6.00; N, 9.26; O, 14.11; S, 7.07. Found: C, 62.68; H, 6.24; N, 8.91; O, 14.79; S, 6.53; Br, 0.84.

2,5-Bis(phenylethynyl)-1,3,4-thiadiazole (7). A mixture of **1** (1.22 g, 5.0 mmol), phenylacetylene (1.12 g, 11.0 mmol), $Pd(PPh_3)_4$ (0.15 g, 0.13 mmol), CuI (0.025 g, 0.13 mmol), dry toluene (15 mL), and dry diisopropylamine (5 mL) was stirred for 12 h at 60 °C under N_2. After cooling to room temperature, the solvent was evaporated. The resulting residue was dissolved in chloroform, and the solution was passed through a short column of Celite. The product was purified with column chromatography (silica, hexane/chloroform = 1:1, v/v). Evaporation and recrystallization from methanol/acetone gave a light-yellow solid of **7** (yield = 0.68 g, 48%). ^{1}H NMR (400 MHz, $CDCl_3$): δ 7.64−7.61 (m, 4H), 7.48−7.39 (m, 6H). ^{13}C{^{1}H} NMR (100 MHz, $CDCl_3$): δ 150.28, 132.13, 130.31, 128.59, 120.44, 99.46, 77.84. FT-IR (KBr, cm^{-1}): 2206, 1494, 1443, 1416, 1261, 1130, 1111, 1072, 999, 927, 765, 757. FAB-MS: *m/z* 287 [M + H]$^+$. Anal. Calcd for $C_{18}H_{10}N_2S$: C, 75.50; H, 3.52; N, 9.78; S, 11.20. Found: C, 75.24; H, 3.68; N, 9.67; S, 10.80.

3,5-Bis(phenylethynyl)-4-propyl-1,2,4-triazole (8). The procedure used to obtain **7** was applied with **2** (0.81 g, 3.0 mmol), phenylacetylene (0.64 g, 6.3 mmol), $Pd(PPh_3)_4$ (0.09 g, 0.08 mmol), and CuI (0.02 g, 0.1 mmol). **8** was obtained as a white solid after purification by column chromatography (silica, chloroform) and recrystallization from methanol (yield = 0.42 g, 45%). ^{1}H NMR (400 MHz, $CDCl_3$): δ 7.61−7.58 (m, 4H), 7.47−7.38 (m, 6H), 4.19 (t, 6.8 Hz, 2H), 1.98 (m, 2H), 1.03 (t, 7.6 Hz, 3H). ^{13}C{^{1}H} NMR (100 MHz, $CDCl_3$): δ 140.31, 131.89, 129.95, 128.57, 120.65, 97.29, 74.64, 47.01, 23.40, 11.23. FT-IR (KBr, cm^{-1}): 3056, 2958, 2873, 2228, 1597, 1515, 1471, 1440, 1421, 1403, 1154, 1070, 998, 924, 902, 764. FAB-MS: *m/z* 312 [M + H]$^+$. Anal. Calcd for $C_{21}H_{17}N_3$: C, 81.00; H, 5.50; N, 13.49. Found: C, 80.78; H, 5.29; N, 13.31.

2,5-Bis(phenylethynyl)-3,4-dinitrothiophene (9). The procedure used to obtain **7** was applied with **4** (1.33 g, 4.0 mmol), phenylacetylene (0.86 g, 8.4 mmol), $Pd(PPh_3)_4$ (0.12 g, 0.1 mmol), and CuI (0.02 g, 0.1 mmol). Triethylamine was used for the reaction instead of diisopropylamine. **9** was obtained as a bright-yellow solid after purification by column chromatography (silica, hexane/chloroform = 1:1, v/v) and recrystallization from methanol/acetone (yield = 0.84 g, 56%). ^{1}H NMR (400 MHz, $CDCl_3$): δ 7.60−7.57 (m, 4H), 7.49−7.39 (m, 6H). ^{13}C{^{1}H} NMR (100 MHz, $CDCl_3$): δ 132.22, 130.66, 128.65, 122.38, 120.31, 105.26, 76.93. FT-IR (KBr, cm^{-1}): 2209, 1549, 1516, 1480, 1442, 1413, 1332, 919, 780, 761. FAB-MS: *m/z* 375 [M + H]$^+$. Anal. Calcd for $C_{20}H_{10}N_2O_4S$: C, 64.16; H, 2.69; N, 7.48; S, 8.57. Found: C, 64.13; H, 2.60; N, 7.55; S, 8.62.

Instruments and Methods. Details for the measurements and quantum-chemical calculations are given in the Supporting Information.

Acknowledgment. The authors are grateful to Professor T. Ikeda and Dr. A. Shishido of our laboratory for their helpful discussions and assistance with the polarized optical microscopy. We also thank Professor T. Kanbara for his valuable advice, Mr. K. Okamoto for his assistance with the X-ray crystallographic analysis, Dr. A. Oiwa for his help and valuable comments for the magnetic susceptibility measurements, and Dr. D. Takeuchi for his kindness in obtaining GPC (THF) traces. We would like to acknowledge to the Global Scientific Information and Computing Center in our institute for generous permission to use the SGI Origin 2000/128. This research was partly supported by a grant for the 21st Century Center of Excellence (COE) program.

Supporting Information Available: Additional experimental details, FT-IR spectra, TGA and DSC thermograms, UV−vis and PL spectra, solvatochromic data, cyclic voltammograms, magnetic susceptibility data of the polymers, table of X-ray crystal data of **7**−**9** (PDF), and crystallographic information files (CIF). This material is available free of charge via the Internet at http://pubs.acs.org.

References and Notes

(1) Reviews: (a) Bunz, U. H. F. *Chem. Rev.* **2000**, *100*, 1605. (b) Bunz, U. H. F. *Acc. Chem. Res.* **2001**, *34*, 998. (c) Moore, J. S. *Acc. Chem. Res.* **1997**, *30*, 402. (d) Ley, K. D.; Schanze, K. S. *Coord. Chem. Rev.* **1998**, *171*, 287. (e) Tour, J. M. *Acc. Chem. Res.* **2000**, *33*, 791. (f) Yamamoto, T. *Bull. Chem. Soc. Jpn.* **1999**, *72*, 621. (g) Yamamoto, T. *Macromol. Rapid Commun.* **2002**, *23*, 583.

(2) (a) Yamamoto, T.; Yamada, W.; Takagi, M.; Kizu, K.; Maruyama, T.; Ooba, N.; Tomaru, S.; Kurihara, T.; Kaino, T.; Kubota, K. *Macromolecules* **1994**, *27*, 6620. (b) Yamamoto, T.; Takagi, M.; Kizu, K.; Maruyama, T.; Kubota, K.; Kanbara, T.; Kurihara, T.; Kaino, T. *J. Chem. Soc., Chem. Commun.* **1993**, 797. (c) Yamamoto, T.; Honda, K.; Ooba, N.; Tomaru, S. *Macromolecules* **1998**, *31*, 7.

(3) (a) Kim, J.; McQuade, D. T.; McHugh, S. K.; Swager, T. M. *Angew. Chem., Int. Ed.* **2000**, *39*, 3868. (b) Yang, J. S.; Swager, T. M. *J. Am. Chem. Soc.* **1998**, *120*, 11864. (c) Zhou, Q.; Swager, T. M. *J. Am. Chem. Soc.* **1995**, *117*, 12593.

(4) (a) Weder, C.; Sarwa, C.; Montali, A.; Batiaansen, C.; Smith, P. *Science* **1998**, *279*, 835. (b) Montali, A.; Batiaansen, C.; Smith, P.; Weder, C. *Nature* **1998**, *392*, 261.

(5) (a) Schmitz, C.; Pösch, P.; Thelakkat, M.; Schmidt, H.-W.; Montali, A.; Feldman, K.; Smith, P.; Weder, C. *Adv. Funct. Mater.* **2001**, *11*, 41. (b) Zhan, X.; Liu, Y.; Yu, G.; Wu, X.; Zhu, D.; Sun, R.; Wang, D.; Epstein, A. J. *J. Mater. Chem.* **2001**, *11*, 1606.

(6) (a) Bumm, L. A.; Arnold, J. J.; Cygan, M. T.; Dunbar, T. D.; Burgin, T. P.; Jones II, L.; Allara, D. L.; Tour, J. M. *Science* **1996**, *271*, 1705. (b) Tour, J. M. *Chem. Rev.* **1996**, *96*, 537. (c) Samorí, P.; Francke, V.; Müllen, K.; Rabe, J. P. *Chem.*−*Eur. J.* **1999**, *5*, 2312. (d) Fan, F.-R. F.; Lai, R. Y.; Cornil, J.; Karzazi, Y.; Brédas, J. L.; Cai, L.; Cheng, L.; Yao, Y.; Price, Jr. D. W.; Dirk, S. M.; Tour, J. M.; Bard, A. J. *J. Am. Chem. Soc.* **2004**, *126*, 2568.

(7) (a) Walters, K. A.; Ley, K. D.; Cavalaheiro, C. S. P.; Miller, S. E.; Gosztola, D.; Wasielewski, M. R.; Bussandri, A. P.; van Willigen, H.; Schanze, K. S. *J. Am. Chem. Soc.* **2001**, *123*, 8329. (b) Egbe, D. A. M.; Klemm, E. *Macromol. Chem. Phys.* **1998**, *199*, 2683.

(8) (a) Yamamoto, T.; Fang, Q.; Morikita, T. *Macromolecules* **2003**, *36*, 4262. (b) Bangcuyo, C. G.; Evans, U.; Myrick, M. L.; Bunz, U. H. F. *Macromolecules* **2001**, *34*, 7592. (c) Morikita, T.; Yamaguchi, I.; Yamamoto, T. *Adv. Mater.* **2001**, *13*, 1862. (d) Yamamoto, T.; Kokubo, H.; Morikita, T. *J. Polym. Sci., Part B: Polym. Phys.* **2001**, *39*, 1713.

(9) (a) Bangcuyo, C. G.; Ellsworth, J. M.; Evans, U.; Myrich, M. L.; Bunz, U. H. F. *Macromolecules* **2003**, *36*, 546. (b) Jégou, G.; Jenekhe, S. A. *Macromolecules* **2001**, *34*, 7926.

(10) (a) Kamiya, M. *Bull. Chem. Soc. Jpn.* **1970**, *43*, 3344 (b) Brocks, G.; Tol, A. *Synth. Met.* **1999**, *101*, 516. (c) Mahanti, M. K. *Indian J. Chem.* **1977**, *15B*, 168. (d) Palmer, M. H.; Simpson, I.; Wheeler, J. R. *Z. Naturforsch* **1981**, *36A*, 1246.
(11) (a) Adachi, C.; Tsutsui, T.; Saito, S. *Appl. Phys. Lett.* **1990**, *56*, 799. (b) Tamoto, N.; Adachi, C.; Nagai, K. *Chem. Mater.* **1997**, *9*, 1077. (c) Kido, J.; Ohtaki, C.; Hongawa, K.; Okuyama, K.; Nagai, K. *Jpn. J. Appl. Phys.* **1993**, *32*, L917. (d) Adachi, C.; Baldo, M. A.; Forrest, S. R.; Thompson, M. E. *Appl. Phys. Lett.* **2000**, *77*, 904.
(12) (a) Huang, W.; Meng, H.; Yu, W.-L.; Gao, J.; Heeger, A. J. *Adv. Mater.* **1998**, *10*, 593. (b) Meng, H.; Yu, W.-L.; Huang, W. *Macromolecules* **1999**, *32*, 8841. (c) Wang, C.; Kilitziraki, M.; Pålsson, L.-O.; Bryce, M. R.; Monkman, A. P.; Samuel, I. D. W. *Adv. Funct. Mater.* **2001**, *11*, 47. (d) Mikroyannidis, J. A.; Spiliopoulos, I. K.; Kasimis, T. S.; Kulkarni, S. A.; Jenekhe, S. A. *Macromolecules* **2003**, *36*, 9295. (e) Kim, J. H.; Park, J. H.; Lee, H. *Chem. Mater.* **2003**, *15*, 3414.
(13) (a) Zhang, Q. T.; Tour, J. M. *J. Am. Chem. Soc.* **1997**, *119*, 5065. (b) Zhang, Q. T.; Tour, J. M. *J. Am. Chem. Soc.* **1998**, *120*, 5355.
(14) (a) Yamamoto, T.; Zhou, Z.-H.; Kanbara, T.; Shimura, M.; Kizu, K.; Maruyama, T.; Nakamura, Y.; Fukuda, T.; Lee, B.-L.; Ooba, N.; Tomaru, S.; Kurihara, T.; Kaino, T.; Kubota, K.; Sasaki, S. *J. Am. Chem. Soc.* **1996**, *118*, 10389. (b) Lee, B.-L.; Yamamoto, T. *Macromolecules* **1999**, *32*, 1375. (c) Zhou, Z.-H.; Maruyama, T.; Kanbara, T.; Ikeda, T.; Ichimura, K.; Yamamoto, T.; Tokuda, K. *J. Chem. Soc., Chem. Commun.* **1991**, 1210.
(15) (a) Havinga, E. E.; Ten Hoeve, W.; Wynberg, H. *Polym. Bull. (Berlin)* **1992**, *28*, 119. (b) Ferraris, J. P.; Bravo, A.; Kim, W.; Hrncir, D. C. *J. Chem. Soc., Chem. Commun.* **1994**, 991. (c) Karikomi, M.; Kitamura, C.; Tanaka, S.; Yamashita, Y. *J. Am. Chem. Soc.* **1995**, *117*, 6791. (d) Kitamura, C.; Tanaka, S.; Yamashita, Y. *Chem. Mater.* **1996**, *8*, 570. (e) Jenekhe, S. A.; Lu, L.; Alam, M. M. *Macromolecules* **2001**, *34*, 7315.
(16) Yamamoto, T.; Kimura, T.; Shiraishi, K. *Macromolecules* **1999**, *32*, 8886.
(17) (a) McCullough, R. D.; Tristram-Nagle, S.; Williams, S. P.; Lowe, R. D.; Jayaraman, M. *J. Am. Chem. Soc.* **1993**, *115*, 4910. (b) Bao, Z.; Dodabalapur, A.; Lovinger, A. J. *Appl. Phys. Lett.* **1996**, *69*, 4108. (c) Sirringhaus, H.; Brown, P. J.; Friend, R. H.; Nielsen, M. M.; Bechgaard, K.; Langeveld-Voss, B. M. W.; Spiering, A. J. H.; Janssen, R. A. J.; Meijer, E. W.; Herwig, P.; de Leeuw, D. M. *Nature* **1999**, *401*, 685. (d) Scherf, U.; List, E. J. W. *Adv. Mater.* **2002**, *14*, 477. (e) Yamamoto, T.; Kokubo, H. *Mol. Cryst. Liq. Cryst.* **2002**, *381*, 1. (f) Yamamoto, T.; Kokubo, H.; Kobashi, M.; Sakai, Y. *Chem. Mater.* **2004**, *16*, 4616.
(18) Yasuda, T.; Imase, T.; Sasaki, S.; Yamamoto, T. *Macromolecules* **2005**, *38*, 1500.
(19) (a) Sanechika, K.; Yamamoto, T.; Yamamoto, A. *Bull. Chem. Soc. Jpn.* **1984**, *57*, 752. (b) Trumbo, D. L.; Marvel, C. S. *J. Polym. Sci., Part A: Polym. Chem.* **1986**, *24*, 2311.
(20) (a) Sonogashira, K.; Tohda, Y.; Hagihara, N. *Tetrahedron Lett.* **1975**, 4467. (b) Dieck, H. A.; Heck, R. F. *J. Organomet. Chem.* **1975**, *93*, 259. (c) Osakada, K.; Sakata, R.; Yamamoto, T. *Organometallics* **1997**, *16*, 5354. (d) Osakada, K.; Sakata, R.; Yamamoto, T. *J. Chem. Soc., Dalton Trans.* **1997**, 1265.
(21) (a) Mangel, T.; Eberhardt, A.; Scherf, U.; Bunz, U. H. F.; Müllen, K. *Macromol. Rapid Commun.* **1995**, *16*, 571. (b) Wautelet, P.; Moroni, M.; Moigne, J. L.; Pham, A.; Biget, J.-Y. *Macromolecules* **1996**, *29*, 446. (c) Erdogan, B.; Song, L.; Wilson, J. N.; Park, J. O.; Srinivasarao, M.; Bunz, U. H. F. *J. Am.Chem. Soc.* **2004**, *126*, 3678.
(22) Kloppenburg, L.; Jones, D.; Claridge, J. B.; zur Loye, H.-C.; Bunz, U. H. F. *Macromolecules* **1999**, *32*, 4460.
(23) Levitus, M.; Schmieder, K.; Ricks, H.; Shimizu, K. D.; Bunz, U. H. F.; Garcia-Garibay, M. A. *J. Am. Chem. Soc.* **2001**, *123*, 4259 and references therein.
(24) (a) Li, H.; Powell, D. R.; Firman, T. K.; West, R. *Macromolecules* **1998**, *31*, 1093. (b) Zhao, L.; Perepichka, I. F.; Türksoy, F.; Batsanov, A. S.; Beeby, A.; Findlay, K. S.; Bryce, M. R. *New J. Chem.* **2004**, *28*, 912. (c) Mavridis, A.; Moustakali-Mavridis, I. *Acta Crystallogr., Sect. B* **1977**, *33*, 3612.
(25) Pillardy, J.; Wawak, R. J.; Arnautova, Y. A.; Czaplewski, C.; Scheraga, H. A. *J. Am. Chem. Soc.* **2000**, *122*, 907.
(26) Yamamoto, T.; Komarudin, D.; Arai, M.; Lee, B.-L.; Suganuma, H.; Asakawa, N.; Inoue, Y.; Kubota, K.; Sasaki, S.; Fukuda, T.; Matsuda, H. *J. Am. Chem. Soc.* **1998**, *120*, 2047.
(27) (a) Jordan, E. F., Jr.; Feldeisen, D. W.; Wrigley, A. N. *J. Polym. Sci., Part A-1* **1971**, *9*, 1835. (b) Hsiech, H. W.; Post, B.; Morawetz, H. *J. Polym. Sci., Polym. Phys.* **1976**, *14*, 1241.
(28) (a) Giesa, R.; Schulz, R. C. *Macromol. Chem.* **1990**, *191*, 857. (b) Davey, A. P.; Elliott, S.; O'Connor, O.; Blau, W. *J. Chem. Soc., Chem. Commun.* **1995**, 1433. (c) Moroni, M.; Moigne, J. L.; Luzzati, S. *Macromolecules* **1994**, *27*, 562.
(29) McQuade, D. T.; Kim, J.; Swager, T. M. *J. Am. Chem. Soc.* **2000**, *122*, 5885.
(30) (a) Li, X.-C.; Kraft, A.; Cervini, R.; Spencer, G. C. W.; Cacialli, F.; Friend, R. H.; Gruener, J.; Holmes, A. B.; DeMello, J. C.; Moratti, S. C. *Mater. Res. Soc. Symp. Proc.* **1996**, *413*, 13. (b) Meng, H.; Huang, W. *J. Org. Chem.* **2000**, *65*, 3894. (c) Ng, S. C.; Ding, M.; Chan, H. S. O.; Yu, W.-L. *Macromol. Chem. Phys.* **2001**, *202*, 8. (d) Huang, W.; Meng, H.; Yu, W.-L.; Gao, J.; Heeger, A. J. *Adv. Mater.* **1998**, *10*, 593.
(31) (a) Yeh, S. J.; Tsai, C. Y.; Huang, C.-Y.; Liou, G.-S.; Cheng, S.-H. *Electrochem. Commun.* **2003**, *5*, 373. (b) Price, D. W. Jr.; Dirk, S. M.; Maya, F.; Tour, J. M. *Tetrahedron* **2003**, *59*, 2497.
(32) (a) Yamamoto, T.; Muramatsu, Y.; Shimizu, T.; Yamada, W. *Macromol. Rapid Commun.* **1998**, *19*, 263. (b) Yamamoto, T.; Muramatsu, Y.; Lee, B.-L.; Kokubo, H.; Sasaki, S.; Hasegawa, M.; Yagi, T.; Kubota, K. *Chem. Mater.* **2003**, *15*, 4384. (c) Muramatsu, Y.; Yamamoto, T. *Chem. Lett.* **1997**, 581.
(33) Brockmann, T. W.; Tour, J. M. *J. Am. Chem. Soc.* **1995**, *117*, 4437.
(34) Coulson, D. R. *Inorg. Synth.* **1972**, *13*, 121.

MA050398P